Confirmation of the Electric Field Gradients at the Nitrogen Nuclei in N-Cyanomethanimine, CH_2NCN, from Low-J Rotational Transitions

W. H. Stolze and D. H. Sutter
Institut für Physikalische Chemie der Universität Kiel

C. Wentrup
Department of Chemistry, University of Brisbane, Brisbane, Australia

Z. Naturforsch. **44 a,** 291–294 (1989); received February 6, 1989

The results of a high resolution microwave study of low-J rotational transitions of N-cyanomethanimine are reported. The ^{14}N quadrupole coupling constants fitted to the observed hyperfine splittings are: $\chi_{aa}(\text{imine}) = 2.032(9)$ MHz, $\chi_{bb}(\text{imine}) = -4.586(7)$ MHz, and $\chi_{aa}(\text{nitrile}) = -3.254(8)$ MHz, $\chi_{bb}(\text{nitrile}) = 0.844(16)$ MHz. Knowledge of these constants together with the rotational constants and centrifugal distortion constants determined earlier provides the basis for accurate prediction of hitherto unmeasured rotational transitions for radioastronomy.

Introduction

Because of its astrophysical interest, the rotational spectrum of N-cyanomethanimine has been studied extensively by Bak et al. at Copenhagen [1–3] and by Winnewisser et al. at Giessen [3, 4]. The latter group has also successfully resolved and analysed the ^{14}N hyperfine structure in the millimeter wave spectrum. The hfs structure is a valuable tool for fingerprint line identification in radioastronomy. However two sets of quadrupole coupling constants were compatible with the observed mm wave spectra, and the authors based the choice of the correct set on the comparison with ab initio field gradients. Now, it turned out recently that present day ab initio methods may still have problems with the calculation of field gradients, especially at a sp^2 hybridized ^{14}N nucleus. We therefore initiated a complementary study of the ^{14}N hyperfine patterns of low-J rotational transitions. These low-J hfs patterns differ sufficiently for the above two sets of coupling constants. Thus an unambiguous experimental determination of the quadrupole coupling constants and the reliable prediction of the hfs patterns also of hitherto unmeasured rotational transitions becomes possible.

Experimental

Since N-cyanomethanimine is highly unstable in the absorption cell (polymerisation), a flow system was set up. The sample was produced immediately before the front end of the cell by flash pyrolysis of trimethylenetetrazole [6] in a quartz tube.

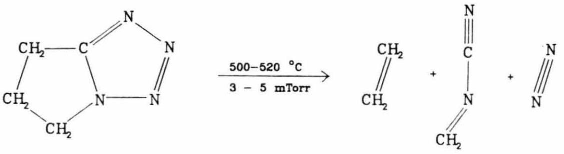

Our quartz tube had an inner diameter of 1 cm. The length of the heated zone was 20 cm. In order to minimize wall collisions the pyrolysis products were fed into the cell coaxially.

Typical total pressures at the front end of the 1.8 m X-band absorption cell were around 10 mTorr and at the rear end around 1 to 3 mTorr. Aluminum waveguide cells proved to be superior to our standard brass waveguide cells. Preconditioning of the system with $CF_3COOC_2H_5$ (as used by Bak and Svanholt in their preparation of the molecule from dimethylcyanamide [2]) improved the signal to noise ratio in the spectra at least by a factor of two.

To record the spectrum, a micro-computer controlled cw-microwave spectrometer with 30 kHz Stark-effect modulation and with phase stabilized backward wave oscillators as radiation sources was

---

Reprint requests to Prof. Dr. D. H. Sutter, Institut für Physikalische Chemie, Universität Kiel, Olshausenstrasse 40, D-2300 Kiel 1.

0932-0784 / 89 / 0400-0291 $ 01.30/0. – Please order a reprint rather than making your own copy.

used. The computer control system, which also provides averaging and data handling capabilities, is described in detail in [7]. Typical experimental linewidths were around 150 kHz full width at half height. In Fig. 1 we present a recording of the 1 0 1 ← 0 0 0 rotational transition since this transition is of special interest for X-band radioastronomy.

Analysis of the ^{14}N Hyperfine Patterns and Discussion

N-cyanomethanimine has a large *a*-component of the electric dipole moment ($\mu_a = 4.7$ D) and a smaller *b*-component ($\mu_b = 1.5$ D) [3]. Thus the *a*-type transition are typically one order of magnitude more intense than the *b*-type transitions. We have therefore selected the four lowest $\Delta J = +1$ *a*-type transitions for our analysis of the ^{14}N-quadrupole hyperfine patterns. Our experimental frequencies are given in Table 1.

The analysis was carried out with our improved version of the computer program Q2SIM [4, 5]. In this program the effective Hamiltonian matrix is set up in the coupled basis $|(JI_1)\, F_1\, I_2\, FM_F\rangle$ (see (2) and (3) of [4]). J, I_1, and I_2 are the angular momentum quantum numbers of the asymmetric top, of the spin of the first (imine) nitrogen, and of the second (nitrile) nitrogen, respectively, i.e. the coupling scheme used is $\boldsymbol{F}_1 = \boldsymbol{J} + \boldsymbol{I}_1$ and $\boldsymbol{F} = \boldsymbol{F}_1 + \boldsymbol{I}_2$. Matrix elements which are off-diagonal in J are neglected. The resulting matrix is diagonalized numerically to obtain the hyperfine energies. The relative intensities of the hfs-satellites are obtained from the corresponding transformation of the electric dipole matrix elements. The program was also extended to include the spin-rotation coupling [8] of the two quadrupole nuclei.

From a least squares fit to the observed splittings, the quadrupole coupling constants presented in Table 2 are obtained. They agree within 40 kHz with solution 1 of [4] (compare too Figs. 2 and 3). Thus the choice by the authors, which had been based on a comparison with ab initio field gradients at the nitrogen nuclei is now also confirmed experimentally. In view of the problems which may arise in present day ab initio calculations especially of field gradients at a sp^2-hybridized nitrogen nucleus ([9] and H.-P. Huber, private comm.), we think that this experimental confirmation was of value. Furthermore, in radioastronomy, the higher accuracy of the coupling constants determined here allows an improved prediction of yet unmeasured quadruople hyperfine patterns.

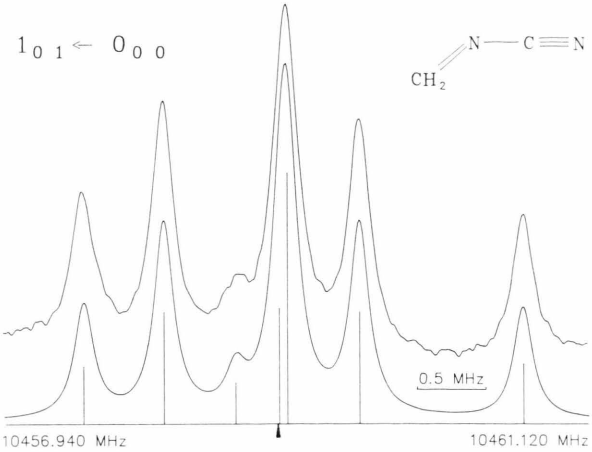

Fig. 1. Recording of the 1 0 1 ← 0 0 0 ^{14}N quadrupole hyperfine pattern of CH_2NCN (upper trace) and the corresponding pattern calculated from the quadrupole coupling constants listed in the first column of Table 2 (lower trace). Lorentzian line shapes with 150 kHz full width at half height were used to calculate the line profile. For the assignment of the satellites see Table 1. Note that the hypothetical center frequency of the multiplet (observed at 10458.898 (4) MHz) was predicted at 10458.8982 MHz from the rotational constants and centrifugal distortion constants determined in the mm wave work [4].

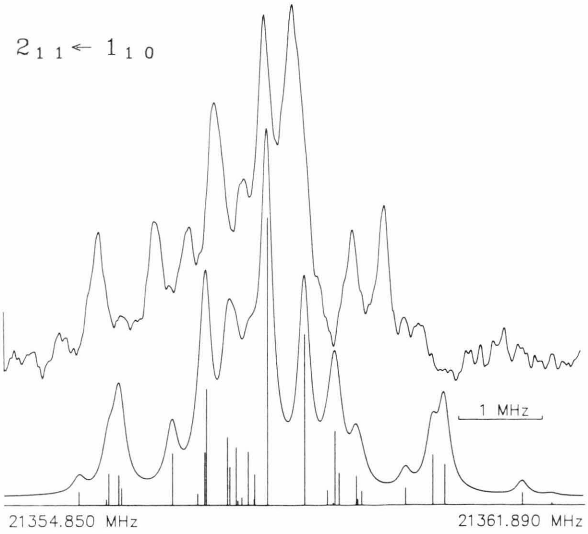

Fig. 2. Recording of the 2 1 1 ← 1 1 0 ^{14}N quadrupole hyperfine pattern of CH_2NCN (upper trace) and hypothetical hyperfine pattern calculated from the second set of quadrupole coupling constants which would also be compatible with the mm wave hyperfine patterns observed in [4]. Due to the obvious discrepancies this set can now be discarded also from the experiment.

Table 1. Measured components of low-J rotational transitions of CH_2NCN split by ^{14}N quadrupole hyperfine interaction. Calculated frequencies result from the optimized coupling constants listed in Table 2. They are calculated under neglect of spin-rotation coupling. For unresolved satellites the last column gives the intensity weighted averages of the calculated frequencies for better comparison with the observed splittings.

$J'\,K'_-\,K'_+ \leftarrow J\,K_-\,K_+$	Unperturbed frequency ν_c (MHz)	$F_1'\,F' \leftarrow$	$F_1\,F$	Rel. int.	Observed frequency (MHz)	$\nu-\nu_c$ obs. (kHz)	$\nu-\nu_c$ calc. (kHz)	$\nu-\nu_c$ aver. (kHz)
1 0 1 ← 0 0 0	10458.898	0 1	1 1	21	10457.509	−1389.	−1379.	−1379.
		0 1	1 2	21			−1379.	
		2 2	1 1	31	10458.079	−819.	−815.	−815.
		2 2	1 2	41			−815.	
		1 0	1 1	15	10458.600	−298.	−306.	−306.
		2 1	1 1	1	10458.947	49.	5.	44.
		2 1	1 0	41			5.	
		2 3	1 2	100			61.	
		1 2	1 1	40	10459.469	571.	571.	571.
		1 2	1 2	31			571.	
		1 1	1 1	20	10460.642	1744.	1741.	1741.
		1 1	1 2	22			1741.	
2 0 2 ← 1 0 1	20915.179	1 1	1 2	3	20913.457	−1722.	−1721.	−1721.
		1 0	1 1	6	20913.840	−1339.	−1427.	−1346.
		1 2	1 2	21			−1324.	
		3 3	2 3	14	20914.240	−939.	−974.	−932.
		3 2	1 1	30			−912.	
		1 1	1 0	10	20914.335	−844.	−845.	−840.
		1 2	2 3	2			−815.	
		2 1	1 1	19	20914.607	−572.	−590.	−588.
		2 2	1 2	1			−556.	
		3 3	2 2	63	20915.210	31.	−98.	31.
		2 2	2 1	54			9.	
		3 4	2 3	100			29.	
		1 2	2 2	3			61.	
		2 3	1 2	65			118.	
		1 1	0 1	18			229.	
		1 2	0 1	29	20915.787	608.	626.	626.
		2 3	2 3	12			627.	
		2 1	1 0	8	20916.647	1468.	1456.	1456.
		3 2	2 2	21	20916.827	1648.	1644.	1654.
		1 0	0 1	5			1693.	
		2 1	2 2	4	20917.139	1960.	1966.	1966.
2 1 1 ← 1 1 0	21358.043	1 1	1 0	6	21355.549	−2494.	−2506.	−2506.
		1 1	1 2	6	21356.000	−2043.	−2134.	−2039.
		1 1	1 1	5			−2023.	
		1 2	1 2	12			−2002.	
		1 0	1 1	4	**	**	−1694.	
		3 3	1 2	18	21356.695	−1348.	−1382.	−1350.
		1 2	2 2	6			−1256.	
		3 2	1 1	17	21357.091	−952.	−948.	−948.
		1 1	2 1	4	21357.408	−635.	−645.	−637.
		3 3	2 2	10			−264.	
		1 2	2 1	19	21357.518	−525.	−513.	−513.
2 1 1 ← 1 1 0	21358.043	3 2	2 2	5	21357.760	−283.	−319.	−283.
		3 3	2 3	10			−264.	
		3 4	2 3	100	21358.024	−19.	−19.	−14.
		2 1	1 0	13			24.	
		2 2	1 2	19	21358.362	319.	191.	314.
		2 2	1 1	26			302.	
		2 3	1 2	34			312.	
		1 1	0 1	12			363.	
		2 1	1 2	3			396.	
		3 2	2 1	17			425.	
		1 2	0 1	16	**	**	495.	
		1 0	0 1	8	**	**	692.	
		2 3	2 2	28	21359.089	1046.	1057.	1057.
		2 3	2 3	16	21359.474	1431.	1429.	1431.
		3 2	0 1	15			1433.	
		2 2	2 1	6	21359.729	1686.	1680.	1680.
		2 1	2 1	10	21359.938	1895.	1885.	1885.
		2 1	0 1	5	**	**	2893.	
2 1 2 ← 1 1 1	20478.541	2 1	0 1	5	20475.619	−2922.	−2930.	−2930.
		3 2	0 1	15	20476.862	−1679.	−1689.	−1689.
		1 1	0 1	14			−1688.	
		1 2	0 1	15	20477.036	−1505.	−1493.	−1485.
		2 2	2 2	6			−1466.	
		2 2	2 1	14	20477.424	−1117.	−1190.	−1130.
		2 3	2 2	14			−1095.	
		1 0	0 1	6			−1068.	
		2 3	2 3	26	20477.634	−907.	−897.	−897.
		2 1	2 1	3	**	**	−731.	
		3 3	2 2	56	20477.975	−566.	−567.	−561.
		2 2	1 2	13	**	**	53.	
		3 4	2 3	100	20478.721	180.	167.	181.
		2 2	1 1	19			215.	
		3 2	2 2	10			235.	
		1 1	2 2	3			237.	
		2 1	1 0	19	**	**	314.	
		2 3	1 2	38	20478.957	416.	423.	424.
		1 2	2 2	4			431.	
		3 2	2 1	12	**	**	510.	
		2 1	1 1	5	20479.241	700.	674.	700.
		1 2	2 1	25			706.	
		3 3	1 2	22	20479.493	952.	957.	957.
		3 2	1 2	4	20480.291	1750.	1753.	1754.
		1 1	1 2	6			1755.	
		3 2	1 1	14	20480.480	1939.	1916.	1926.
		1 1	1 1	11			1917.	
		1 2	1 2	10			1949.	
		1 0	1 1	5	**	**	2537.	

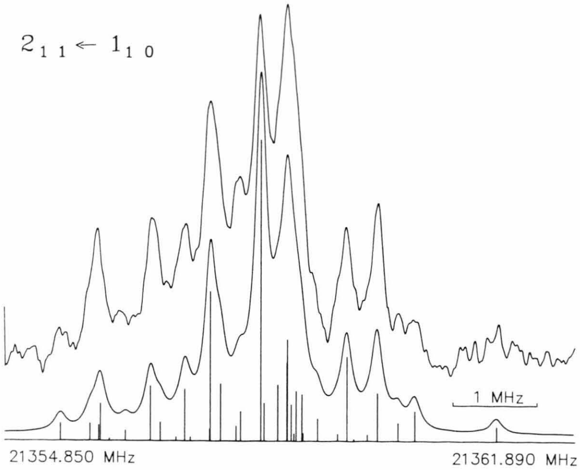

Fig. 3. Recording of the 2 1 1 ← 1 1 0 ^{14}N quadrupole hyperfine pattern of CH_2NCN (upper trace) and the hyperfine pattern calculated from the quadrupole coupling constants listed in the first column of Table 2. The line profile was calculated assuming Lorentzian lineshapes with 150 kHz full width at half height for the satellites. For the assignment of the satellites see Table 1.

Table 2. ^{14}N quadrupole coupling constants of the imine nitrogen and the nitrile nitrogen in CH_2NCN. The rotational constants, which enter into the calculation of the hyperfine splittings, were taken from ref. [4]. They are:

$$A = 63372.995\text{ MHz},\quad B = 5449.3479\text{ MHz},\quad\text{and}\quad C = 5009.5599\text{ MHz}.$$

Two sets of constants are presented. The first constants are presented. The first column gives the fit under neglect of nitrogen spin-rotation coupling, the second column gives the fit including nitrogen spin-rotation coupling. With high relative uncertainties, the spin-rotation coupling constants are essentially undetermined. For future prediction of yet unmeasured hyperfine patterns we therefore recommend the use of the data in the first column.

X_{aa} (imine) / MHz	2.032 (9)	2.035 (10)
X_{bb} (imine) / MHz	−4.586 (7)	−4.589 (13)
X_{cc} (imine) / MHz	2.554 (9)	2.554 (13)
X_{aa} (nitrile) / MHz	−3.254 (8)	−3.251 (8)
X_{bb} (nitrile) / MHz	0.844 (16)	0.842 (17)
X_{cc} (nitrile) / MHz	2.410 (16)	2.409 (17)
c_{aa} (imine) / MHz		−0.002 (7)
c_{bb} (imine) / MHz		−0.001 (3)
c_{cc} (imine) / MHz		0.001 (5)
c_{aa} (nitrile) / MHz		−0.007 (8)
c_{bb} (nitrile) / MHz		0.004 (4)
c_{cc} (nitrile) / MHz		0.002 (5)

Acknowledgements

The authors would like to thank M. Palmer and H.-P. Huber for stimulating discussions on ab initio calculations of nitrogen field gradients and the members of the machineshop of the Kiel institute for manufacturing the absorption cell and the special gas inlet system. We are also grateful to M. and B. Winnewisser for making the program Q2SIM available to us. Support by the Deutsche Forschungsgemeinschaft under grant Su 41/12 and from the Fonds der Chemischen Industrie is gratefully acknowledged.

[1] B. Bak, O. J. Nielsen, and H. Svanholt, Chem. Phys. Letters **59,** 330 (1978).
[2] B. Bak and H. Svanholt, Chem. Phys. Letters **66,** 387 (1979).
[3] B. Bak and H. Svanholt, Chem. Phys. Letters **75,** 528 (1980).
[4] M. Winnewisser, B. Winnewisser, and C. Wentrup, J. Molec. Spectrosc. **105,** 193 (1984).
[5] M. Winnewisser, B. Winnewisser, and C. Wentrup, J. Molec. Spectrosc. **107,** 212 (1984).
[6] C. Wentrup, Tetrahedron **27,** 1281 (1971).
[7] W. H. Stolze, Dissertation, Kiel 1988.
[8] W. Gordy and R. L. Cook, Microwave Molecular Spectra, Intersc. Publ., New York 1970, p. 809.
[9] L. Albinus, J. Spieckermann, and D. H. Sutter, J. Molec. Spectrosc. **133,** 128 (1989).